

**MEASUREMENT OF INTACT-CORE LENGTH  
OF ATOMIZING LIQUID JETS BY IMAGE DECONVOLUTION**Roger Woodward, Robert Burch, Kenneth Kuo, and Fan-Bill Cheung  
Propulsion Engineering Research Center

and

Department of Mechanical Engineering  
The Pennsylvania State University  
University Park, PA 16802**SUMMARY:**

The investigation of liquid jet breakup and spray development is critical to the understanding of combustion phenomena in liquid-propellant rocket engines. Much work has been done to characterize low-speed liquid jet breakup and dilute sprays, but atomizing jets and dense sprays have yielded few quantitative measurements due to their high liquid load fractions and hence their optical opacity. This work focuses on a characteristic of the primary breakup process of round liquid jets, namely the length of the intact-liquid core. The specific application considered is that of shear-coaxial-type rocket engine injectors in which liquid oxygen is injected through the center post while high-velocity gaseous hydrogen is injected through a concentric annulus, providing a shear force to the liquid jet surface. Real-time x-ray radiography, capable of imaging through the dense two-phase region surrounding the liquid core, is used to make the measurements. The intact-liquid-core length data have been obtained and interpreted using two conceptually different methods to illustrate the effects of chamber pressure, gas-to-liquid momentum ratio, and cavitation.

**TECHNICAL DISCUSSION:**

The focus of this study is the measurement of the intact-core length of coaxial jets using X-ray radiography. Two injector sizes are used, having liquid exit diameters and annular-gas-flow exit areas of 1) 4.8 mm (3/16 in) and 45 mm<sup>2</sup> (0.069 in<sup>2</sup>) and 2) 2.4 mm (3/32 in) and 11 mm<sup>2</sup> (0.017 in<sup>2</sup>). The propellant simulants consist of a solution of potassium iodide (KI) in water for the LOX and gaseous nitrogen or helium for the annular-flowing hydrogen. Iodide is a X-ray absorber, thus allowing of line-of-sight imaging of the spray. A detailed description of the test and image processing equipment, setup, and calibration has been given previously (1-3). Following Beer's law, the measured radiance levels of the resulting image are a function of liquid thickness. Through the use of calibration cells, the integrated liquid thickness at each point in the jet can be obtained.

In the course of this study, two different methods of data analysis have been used to determine the intact core length from the X-ray images: a threshold criterion technique based on the integrated liquid thickness, and a threshold criterion based on mean liquid volume fraction using a deconvolution technique. In previous studies by this research group [1-3], the intact-core length was obtained from the processed images using a threshold value based on an integrated liquid thickness corresponding to the end of the intact core. The threshold criterion was selected to be the mean radiance of the 1.6 mm calibration cell for the larger injector and for the smaller injector, a radiance level corresponding to one-fourth that thickness. The core length was measured directly from the image for each of ten

images corresponding to that one flow condition. These measurements were then averaged for one mean value at each condition. Figure 1 presents dimensionless intact-core length ( $L_b/D$ ) results obtained using this image threshold technique versus dimensionless chamber pressure for a range of gas velocities and two sets of liquid velocities ( $v_l = 15$  and  $27$  m/s). Figure 2 presents similar results for the smaller injector over a range of gas velocities and two sets of liquid velocities ( $v_l = 30$  and  $60$  m/s). These results are discussed in detail by Woodward [3].

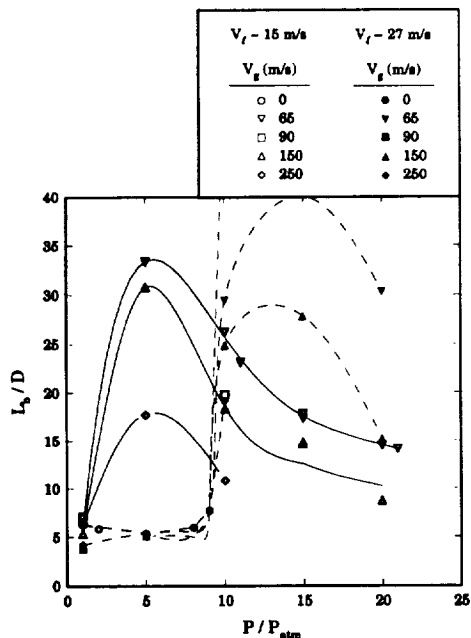


Figure 1. Effect of chamber pressure (gas density) on intact-core length for larger injector using liquid thickness threshold criterion length.

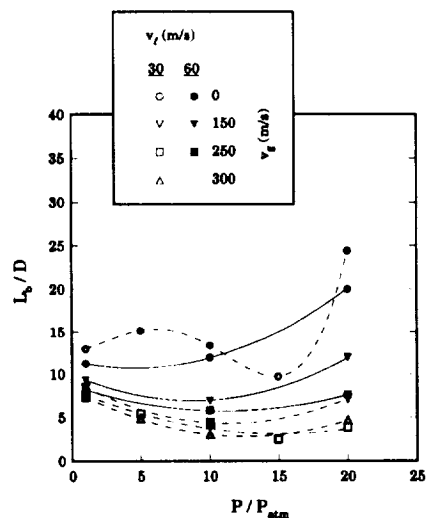


Figure 2. Effect of chamber pressure on intact-core length for injector B (smaller injector).

The selection of the aforementioned threshold criterion is somewhat arbitrary since it is based on an integrated liquid thickness over the entire jet cross section and not an actual core diameter (although such a technique is largely dependent on the core diameter). The alternate technique, based on image deconvolution, considers the combined x-ray path length through the gas as well as the liquid, accounting for the two-phase regions of the coaxial spray. This technique requires the following assumptions to determine radial distributions of the mean liquid volume fraction: axial symmetry of the jet and statistically steady flow. The 33 ms exposures used are of a sufficient length of time for the jet to adequately meet these assumptions. The time-averaged intact-liquid-core and the radial boundary is demarcated by the departure from unity of the liquid volume fraction.

As recommended by Dasch [4], to accomplish the jet image deconvolutions, the three-point Abel inversion has been applied to the present problem since it is relatively easy to calculate and was shown to be more robust and less noisy in controlled tests cases than other common methods. All deconvolution techniques are very sensitive to noise present in the original line-of-sight projection data. To improve the smoothness of the x-ray absorption profiles across the liquid jet in the normalized injection images, the entire series of ten images per test case is averaged together to create one clean normalized image at that injection condition; and lastly, a spatial smoothing is applied to this averaged image.

To determine mean liquid volume fractions, which by definition vary from zero to unity, the deconvolution results are normalized by centerline results very near the injector exit where the liquid volume fraction is at least approximately unity. The intact-liquid-core length is determined for each image by thresholding the resultant deconvoluted-jet image at a mean liquid volume fraction value of 0.9. The core length is then measured in terms of pixels directly from this image.

Figure 3 presents the intact-core length results obtained from jet image deconvolutions for tests conducted with the larger injector. Dimensionless core length is plotted versus dimensionless chamber pressure. As in Fig. 1, two sets of liquid jet velocity data ( $v_\ell=15$  and  $27$  m/s) are represented. It is apparent from Fig. 3 that the core-length curves representing constant gas and liquid velocity have a shape and trend very similar to their threshold technique counterparts in Fig. 1. However, since these figures being compared are plotted at the same scale, it is obvious that the results obtained from the jet image deconvolutions are considerably shorter than those obtained using the threshold technique. The reduction in intact-core length compared to the previous results is not of a constant factor. On average for the results reported in Fig. 3, the intact-core lengths from the deconvoluted jet images are 40% shorter than those obtained using the threshold technique with the 1.59 mm (1/16 in.) threshold criterion. This reduction factor varies over a range of 20% to nearly 70% for one extreme case. Although the intact-core measurements resulting from the determination of liquid volume fraction distributions are much shorter than the corresponding results from the threshold method, the single jet tests in the non-cavitating regime (at  $P_C = 4$  atm and above for  $v_\ell \approx 15$  m/s and at  $P_C = 10$  atm and above for  $v_\ell \approx 27$  m/s) still indicate off-scale ( $> 30$  liquid exit diameters) core lengths. On the other hand, the  $v_\ell = 30$  m/s,  $v_g = 65$  m/s core length result at an ambient pressure condition of 15 atm that was previously off-scale now shows a measurable intact length of 19.8 injector diameters.

Although the deconvolution results presented in Fig. 3 match in general the breakup length trends exhibited by the corresponding threshold method results, there is one data point that shows a major discrepancy. The point at 15 atm on the  $v_\ell \approx 27$  m/s,  $v_g \approx 150$  m/s curve is below its neighboring points at 10 and 20 atm. Based on the other  $v_\ell \approx 27$  m/s curve of Fig. 3 and the corresponding results of Fig. 1, the 15 atm point in question should be near the peak of the curve. Also, the  $v_\ell \approx 15$  m/s,  $v_g \approx 65$  m/s data point lies above the higher liquid velocity point as shown so that another disagreement occurs with the reasoning that the larger liquid jet momentum associated with the higher jet velocity should result in a longer intact core length. It is suspected that this stray data point is an anomaly and that previous findings should not be refuted by this.

Analogous to Fig. 3, Fig. 4 is a plot of the intact-core-length-via-deconvolution results obtained this time using the smaller injector. While Fig. 3 appeared as a squashed but similar version of the corresponding threshold results, Fig. 4 bears little resemblance to the corresponding threshold technique results in Fig. 2. Some of the indicated core lengths are shorter and some are longer than their counterparts determined by the previous method. No consistent trend is exhibited by these deconvolution results for the smaller injector. It is likely that the measurement of intact-core length by the deconvolution method is more unreliable for the smaller injector. This is quite conceivable considering the lower x-ray attenuation levels associated with the smaller diameter jet and the fact that there are only a few pixels across the liquid jet. The spatial resolution as well as the gray level resolution may be

insufficient to produce a decent deconvolution of the smaller jet, especially considering that the injection images of the smaller injector are subject to the same noise levels seen in the larger injector images.

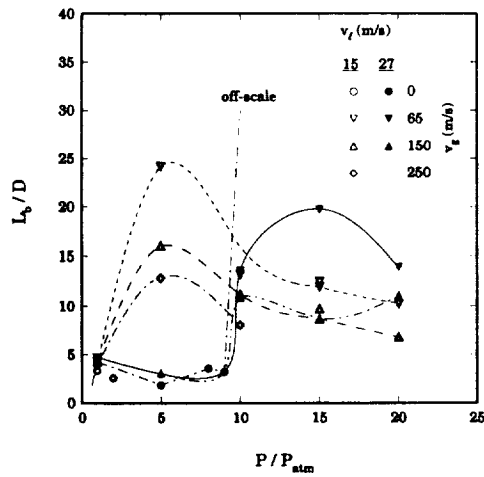


Figure 3. Intact-core length results obtained using the image deconvolution method for injector A tests.

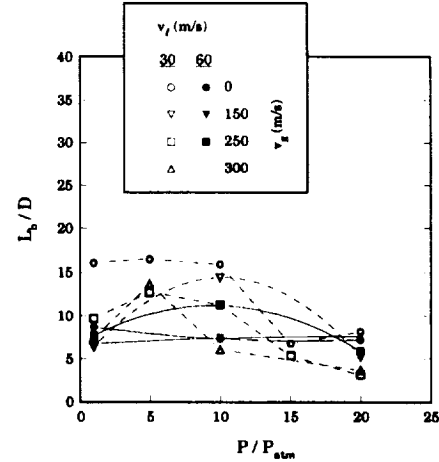


Figure 4. Intact-core length results obtained using the image deconvolution method for injector B tests.

Two conceptually different methods have been used to determine intact-liquid-core lengths for coaxial injection at realistic flow rate conditions: 1) thresholding of jet images to reveal the core region corresponding to a specified liquid integrated thickness and 2) deconvolution of time-averaged jet images to get mean liquid volume fraction distributions. Intact-core results between these two methods agree in form but not in magnitude. Theoretically, the deconvolution method is the more correct one to use; however, it is difficult to obtain an accurate deconvolution due to sensitivity to noise in the line-of-sight image data. Hence, the intact-core lengths obtained using this method are of uncertain accuracy and even questionable for the smaller injector. The threshold technique was applied to the larger injector by using a 1.59 mm (1/16 in.) integrated liquid thickness as the criterion to determine the extent of the core. The consistently shorter deconvolution results indicate that this criterion thickness may be too thin. A major problem with the threshold technique is that different thickness criteria are needed for different size injectors.

#### REFERENCES:

- 1 Woodward, R. D., Burch R. L., Kline M. C., Kuo, K. K., and Cheung, F.-B., "Measurement of Intact-Liquid-Core Length of Rocket Engine Coaxial Injectors," Fourth Annual PERC Symposium, NASA-MSFC, Huntsville, AL, September 1992.
- 2 Woodward, R. D., Burch R. L., Kuo, K. K., and Cheung, F.-B., "Real-Time X-Ray Radiography Study of Liquid Jet Breakup from Rocket Engine Coaxial Injectors," The Third International Symposium of Special Topics in Chemical Propulsion: Non-Intrusive Combustion Diagnostics, Scheveningen, The Netherlands, May 1993.
- 3 Woodward, R. D., Primary Atomization of Liquid Jets Issuing from Rocket Engine Coaxial Injectors, Ph.D. Thesis, The Pennsylvania State University, Aug. 1993.
- 4 Dasch, C. J., "One-Dimensional Tomography: A Comparison of Abel, Onion-Peeling, and Filtered Backprojection Methods," *Applied Optics*, Vol. 31, No. 8, March 1992, pp. 1146-1152.